Hydrogen Jet fires in a full-scale road tunnel: Experimental results

Etienne Studer, Diana Forero, Sergey Kudriakov, Gilles Bernard-Michel, Didier Bouix, François Sauzedde

Hydrogen Jet fires in a full-scale road tunnel: Experimental results

E. Studer[1], D. Forero[1], S. Kudriakov[1], G. Bernard-Michel[1], D. Bouix[2], F. Sauzedde[2]

[1] Univ. Paris-Saclay, CEA, ISAS, F-91191 Gif-sur-Yvette, France
[2] Univ. Grenoble Alpes, CEA, LITEN, F-38000 Grenoble, France

***Corresponding author*: etienne.studer@cea.fr**

ABSTRACT

Hydrogen Fuel Cell Electric Vehicles (HFC EVs) represent an alternative to replace current internal combustion engine vehicles. The use of these vehicles with storage of compressed gaseous hydrogen (CGH2) or cryogenic liquid hydrogen (LH2) in confined spaces, such as tunnels, underground car parks, etc., creates new challenges to ensure the protection of people and property and to keep the risk at an acceptable level. Several studies have shown that confinement or congestion can lead to severe accidental consequences compared to accidents in an open atmosphere. It is therefore necessary to develop validated hazard and risk assessment tools for the behaviour of hydrogen in tunnels. The HYTUNNEL-CS project sponsored by the FCH-JU pursues this objective. Among the experiments carried out in support of the validation of the hydrogen safety tools, the CEA conducted tests on large-scale jet fires in a full-scale tunnel geometry.

The tests were performed in a decommissioned road tunnel in two campaigns. The first one with 50 liters type II tanks under a pressure of 20 MPa and the second one with 78 liters type IV tanks under 70 MPa. In both cases, a flate plate was used to simulate the vehicle. Downward and upward gas discharges to simulate a rollover have been investigated with various release diameters. For the downward discharge, the orientation varied from normal to the road to a 45° rearward inclination. The first campaign took place under a concrete vault while the second under a rocky vault. Additional tests with the presence of a propane fire simulating a hydrocarbon powered vehicle fire were performed to study the interaction between the two reactive zones.

In the paper, all the results obtained during the second campaign for the evolution of the hydrogen jet-fire size, the radiated heat fluxes and the temperature of the hot gases released in the tunnel are reported. Comparisons with the classical correlations from open field tests used in engineering models are also presented and conclusions are given as to their applicability.

1.0 Introduction

Hydrogen Fuel Cell Electric Vehicles (HFC EVs) powered by pressurized hydrogen gas can be involved in a traffic accident with a conventional vehicle with a gasoline internal combustion engine leading to a gasoline pool fire. For the hydrogen vehicle, the approaching fire will cause the temperature around the tank to rise and activate the relief valve (thermally activated pressure relief valve TPRD) at about 110°C. Then, tank depressurizes avoiding its catastrophic rupture if it were engulfed in the fire. When the valve is opened, hydrogen in contact with air ignites and a jet-fire develops while the tank empties. The diameter of the TPRD has evolved from 5 to 6 mm at the beginning to around 2 to 3 mm today leading to a longer duration but shorter flames. The exhaust of the TPRD is usually below the vehicle and directed downwards. If the vehicle has rolled over after the accident, horizontal or vertical upward discharges must also be considered.

The behaviour, dynamics and characteristics of hydrogen jet-fires are described in detail in the 2013 publication by Molkov [1]. Numerous tests have been performed to characterize these turbulent under-expanded flames with driving pressures up to 90 MPa and TPRD diameters D from 0.4 to 50mm [2]–

[4]. Generally, the information reported in these tests are the geometrical characteristics of the flame (length, width, and shape), temperature measurements in the hot gases and radiative fluxes. For the length of the flame L_F, Molkov proposes a correlation:

$$\frac{L_F}{D} = 805\left(\frac{\rho_N}{\rho_\infty} Ma_N^3\right)^{0.47} \quad (1)$$

where ρ is the density, Ma the Mach number and subscripts N refers to the nozzle and ∞ to the surrounding atmosphere.

Hydrogen flames emit mainly in the UV and IR ranges [5] and excited-state water molecules are responsible for these emissions [6]. The fraction of the total power radiated by the hydrogen flame X_{rad} is between 4 and 10% [2], which is about half that of a natural gas flame [7] because of less wavelengths in its products [8]. The rest of heat release is convected with the hot burnt gases. The radiated fraction has a logarithmic dependence on the residence time in the flame as for hydrocarbon flames [2]. Simplified models have been built to evaluate the emitted radiative flux [2], [9] and to predict the radiative flux ϕ_{rad} received at different distances. For the far field, a point source model is relevant, whereas for the near field, a multi-source model [10] or a solid flame model [11] are more consistent with the experimental results.

CFD models are used to predict the behaviour of jet-fires. They are based on "notional nozzle" to represent the TPRD and do not describe in detail the connection zone between the sonic flow from the TPRD and the subsonic zone located downstream. Then, the turbulence model is based on the transport of two variables, generally the turbulent kinetic energy k and its dissipation ε with an Eddy-Dissipation Model (EDM) for combustion modelling whose characteristic time is that of the turbulent mixing k/ε. Finally, for the radiation part, the models of the radiative transfer equation (RTE) vary from a simplified homogeneous approach (P1 harmonic) to a Monte-Carlo treatment. Generally, the flame dimensions and temperatures are well predicted whereas the radiated fluxes are more difficult to capture [12], [13].

For the safety of goods and people, the flame and the hot burnt gases have a direct impact. Indirect effects can also be induced by the radiated heat fluxes and lead to burns of various degrees for people. The effects are expressed in terms of radiated heat flux or thermal dose TD defined as:

$$TD = \int_0^t (\varphi_{rad})^{4/3} dt \quad (2)$$

The Table 1 from [12] gives commonly accepted reference values for these indirect effects.

Table 1. Harm criteria for indirect effects of jet-fires.

	Radiated heat flux (kW/m²)	**Thermal dose ((kW/m²)$^{4/3}$.s)**
No harm	1.6	
First degree burn	4	80-130
Second degree burn	9.5 (t > 20s)	240-730
Third degree burn	25 (t>8s)	870-2640
100% lethality	25 (t>1min)	~5000

Large-scale hydrogen jet-fire tests have generally been conducted in open fields. However, the accident can also take place in a confined environment such as a tunnel or an underground parking lot, the former generally leading to more violent accidents due to the higher speed. In this situation, the confinement

will influence the development of the jet-fire and modify the interaction with the initiating fire. In addition, the added-power released by the jet-fire can affect the circulation of hot gases throughout the tunnel e.g. the back-layering phenomenon [14].

Several studies have shown that confinement or congestion can lead to severe accidental consequences compared to accidents in an open atmosphere. It is therefore necessary to develop validated hazard and risk assessment tools for the behavior of hydrogen in tunnels. The HyTunnel-CS (https://hytunnel.net/) project sponsored by the FCH-JU pursues this objective. Among the experiments carried out in support of the validation, the CEA has conducted tests on Jet-Fire and Fire/Jet-Fire interaction in a full-scale tunnel geometry.

The tests were organized in two phases. The first one in October 2020 in which type II hydrogen cylinders under 20 MPa were used [15]. The second in June 2021 in which type IV tanks of 78 liters under 70 MPa were studied. In these tests, in addition to the effect of the internal pressure, the effect of the diameter of the release and its orientation was investigated on the jet-fire geometry, hot gases cloud transport and radiated heat fluxes in the tunnel. Additionally, effect of the presence of the nearby car-fire was also investigated by the use of a propane burner.

It should be noted that for 2021 tests, TPRD correspond to a manufactured TPRD with a passage aperture as a calibrated orifice and not to a commercially available system as for the 2020 tests.

The paper is organized as follows. In a first section, the geometry used for the test is briefly described. Then, the different phases of the test and the test matrix are detailed. Finally, the results are provided for the behavior of the jet-fire mainly for the 2021 test series. Conclusions and recommendations follow.

2.0 Test geometry

A schematic description of the test arrangement is provided in Figure 1. The first configuration corresponds to jet-fire tests while the second describes the interaction between a car fire and the same jet-fire. The tests were performed in the “tunnel du Mortier” (near Autrans village, Isère, France). This disused road tunnel is a horse-shoe type geometry with a total length of about 502 m. The slope is 3.6% and the tunnel is divided in two different sections. The one located on the Autrans side is made of a flat concrete ceiling arch and the second one on the Montaud side is raw limestone rocks. The injection device was installed in this second section for the 2021 tests whereas for the 2020 tests it was located in the concrete section.

The tunnel dimensions vary in the rocky section, an average height is close to 5.9 m, and the diameter is about 8.9 m. Two sidewalks are also present on each side of the road. The chassis, a flat plate (1.9x5.5m) representing a real car is parallel to the road. The calibrated orifice representing the thermally activated relief device (TPRD) of a real compressed gaseous hydrogen storage is located at the rear of the chassis (230 mm above the road) and it can be oriented upward (UP), downward (DW) with two angles (90° and 45° to the rear). The angles are counted from the chassis which means that 90° does not correspond to the vertical because of the slope of the tunnel.

2.1 Measurement devices

The monitoring system used 100 Hz data acquisition frequency and it can be divided into two parts:

- The one related to the injection tank and the release pipes. Relative pressures and gas temperature were recorded inside the tank (P_0, T_0), at the outlet of the tank (P_1, T_1) and upstream the calibrated orifice (P_2, P_{2bis} and T_2). These were used to check the mass balance and compute the release flowrate.

- The one related to the tunnel. 10 vertical masts were used to support the main measuring devices in the upper part of the tunnel. Additional supporting structures were installed around the chassis

on the lower part to monitor the radiated heat fluxes (labelled *Fx*). These sensors were mainly hydrogen concentration measurement (*Xe* and *He* catharometers) and Type K thermocouples (*Tk*). Oxygen concentration sensors (*Ox*) and CO_2 sensors (*CO2*) were also installed to study possible depletion of oxidizer and production of CO_2 by the propane burner. Ultrasonic wind sensors monitored the convection flow in the tunnel during the tests.

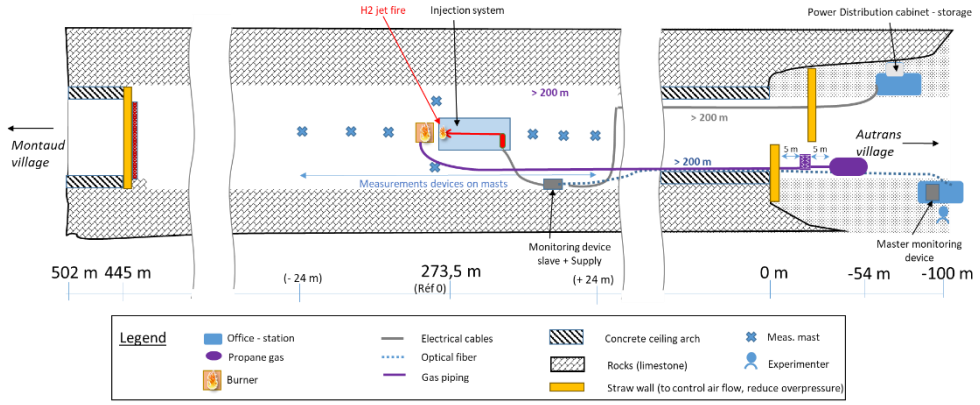

Figure 1. General sketch of the 2021 jet/fire and fire/jet-fire interaction tests.

In the 2020 tests, a supporting structure was placed facing the TPRD injection, where eight staggered Captec radiometers were installed (Figure 2 a). In the 2021 test series, the same sensors were installed during the jet-fire and the burner tests. Four of them were arranged on a similar structure (Figure 2 b) facing the vertical jet-fire. The other four were arranged on single vertical masts (Figure 2 c) and can be moved from tests to tests depending on the fire location. The location of sensors are given by x in the width of the tunnel, y along the axis of the tunnel and the elevation z coordinates where (0, 0, 0) corresponds in both test series at the TPRD exit center in the upward release configuration.

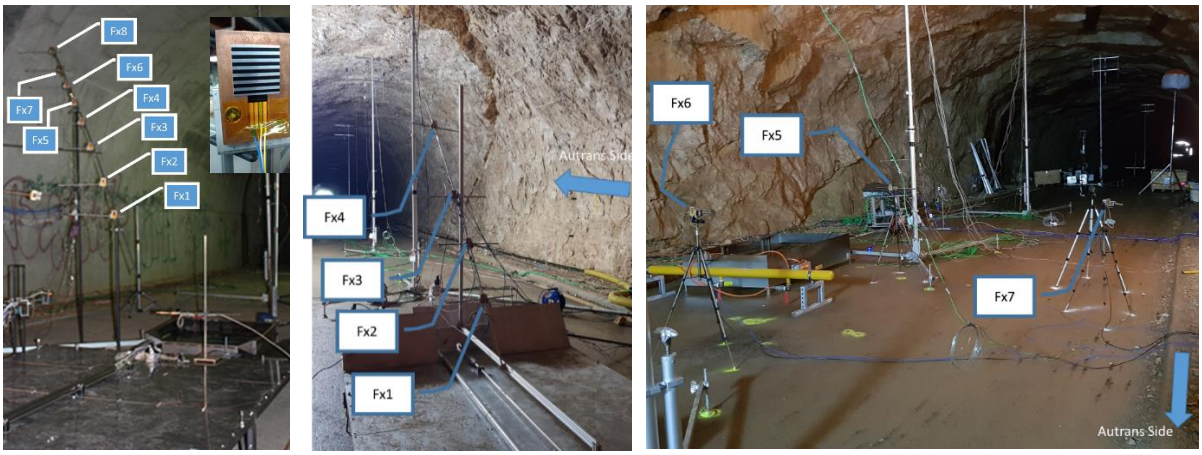

a) b) c)

Figure 2. Radiative heat flux sensors: a) 2020 test series, b) 2021 test series – structure with 4 staggered sensors, c) 2021 test series – Example of single sensors arrangement (tests 21-09 and 21-10).

2.2 Description of the burner

The propane burner (Figure 3 a) was designed with two zones to simulate a localized and an engulfing fire. The dimensions of the ramps are: for the localized fire 300x900 mm with 9 pipes, and for the engulfing fire 1340x900 mm with 43 pipes.

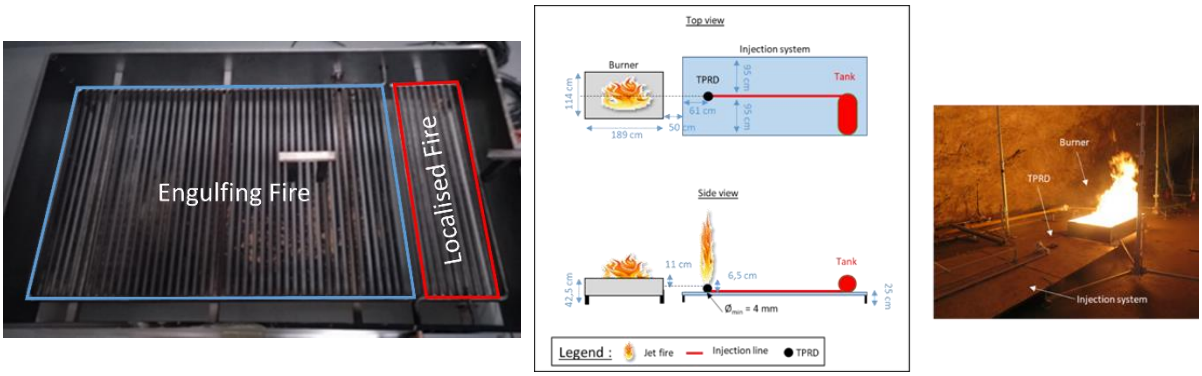

a) b)

Figure 3. Burner: a) Picture of the two zones: left – engulfing area, right – localized area and b) Position of the burner in the tunnel.

The pipes have an outer diameter (O.D.) of 16 mm and a thickness of 1 mm. They are made of stainless steel 304L. The spacing between pipes is 30 mm and the upper holes have a diameter of 1.5 mm and are located every 30 mm. A single tube of 21.3 mm O.D. and 1.3 mm thickness feeds each burner. The ramps are installed in a box (353 mm height for the surrounding plate and 80 mm for the 4 supporting tubes located at the four corners) and located 310 mm above the floor. The burner is fed by a propane tank at a given supply pressure to achieve a heat release rate (HRR) close to 1 MW/m². Ulster University has provided two propane mass flowrates to satisfy the requested HRR: 4.2 g/s for the localized fire and 23.4 g/s for the engulfing fire. For the interaction tests, the two sections of the burner were ignited at the maximum flowrate. The position of the burner in the tunnel relative to the jet fire is depicted in Figure 3 b.

3.0 Test sequence and test matrix

The test sequence is divided into several steps:

- Step 1: connection of the tank to the injection system, opening of the main tank valve to pressurize the pipe between the tank and the solenoid valve, control of the leak tightness;
- Step 2: ignition of the pilot flame used to ignite the jet-fire;
- Step 3: ignition of the burner (if required) for several minutes;
- Step 4: opening of the solenoid valve of the tank to release hydrogen;
- Step 5: closure of the solenoid valve and continuation of the measurements.

Time zero was set to the beginning of Step 4.

In this article, the results of the 2021 tests are mainly described (Table 2). As a reminder, the 2020 tests were performed with a type II tank and pressure limited to 20 MPa and a volume of 50 liters and presented in [15]. The first test of the 2021 campaign (Test 21-09) was therefore intended to reproduce a reference jet-fire under the conditions of 2020 (Test n°20-17)[15] but under the rocky vault. Then, the comparison between the results of tests 21-09 and 21-10 enabled to quantify the effect of the increase in storage pressure and of larger quantities. Comparison between tests 21-10 and 21-18 allowed quantifying the effect of release location. For downward release, the effect of orientation (45 or 90°) can be assessed by comparing the results of test 21-12 with the ones of test 21-18. Finally, the effect of release diameter for a downward release of 45° was investigated by comparing tests 21-12 and 21-13.

A jet fire from a TPRD initiation in a confined space may have a twofold effect on a vehicle fire consequences. The hydrogen jet fire may significantly increase the heat release rate. And, the water vapour produced by H_2-air combustion or the oxidizer depletion may counteract as an extinguisher of the fire. The interaction tests were conducted with these objectives. Comparisons between test 21-14, test 21-15 and test 21-10 allowed the quantification of these effects for a 2 mm release upwards.

Table 2. Jet-fire and Fire/Jet-fire interaction test matrix.

Type of test	Nb of test	Volume (liter)	Pressure (MPa)	Configuration	Ø TPRD (mm)	C_d	Max Flowrate (g/s)	Test number
H2 jet fire (2021)	5	50 type II	17.7	UP	2	0.75	25	n°21-09
		78 Type IV	59.8	UP	2	0.75	68	n°21-10
			63.5	DW 45°	2	0.78	72	n°21-12
			66.3	DW 45°	1	0.93	28	n°21-13
			66.7	DW 90°	2	0.85	77	n°21-18
Burner (2021)	1	-	-	-	-	-	-	n°21-14
H2 jet fire + burner (2021)	1	78 Type IV	66.1	UP	2	0.78	73	n°21-15

4.0 Results and discussions

4.1 Blowdown characterization

Before analysing jet-fire results, the tank blowdown has to be characterized to get the mass flowrate because no direct measurement were performed. Hence, these data were required to compare the results with the engineering correlations mentioned above. Two methods were used:

- **The mass balance method (MBM):** the data of temperature and pressure sensors located close to the On Tank Valve (T_1-P_0 or T_1-P_1) are used to compute the density of the gas (ρ_{gas}) using Abel-Noble equation of state. T_0 is not used in the computation because of the high thermal inertia of the sensor already installed by the tank manufacturer. The mass of gas in the tank is then computed using the obtained density and the volume of the tank (V_{tank}). In a second step, the mass flow rate Q_{MBM} is computed using the first derivative of the mass balance method for the complete duration of the blowdown period.

$$m_{gas} = \rho_{gas}(T, P)V_{tank} \quad (3)$$

$$Q_{MBM} = \frac{\Delta m_{gas}}{\Delta t} \quad (4)$$

- **The sonic nozzle method (SNM)**: in this method, the temperature and pressure values from the sensors close to the TPRD are used (T_2-P_2 or T_2-P_{2bis}). This method uses the theoretical model "Barré de Saint Venant" to compute the mass flow for a sonic regime Q_{SNM}, which is encountered at the exit of the TPRD if the pressure is above the critical one. The geometry and the surface roughness of the nozzle are not considered in this method and a correction is then introduced through a discharge coefficient (C_d).

$$Q_{SNM} = C_d\left(\frac{\pi D^2}{4}\right)\sqrt{\frac{2\gamma r\rho_N^2 T_2}{(\gamma-1)+2(1-b\rho_N)^2}} \quad (5)$$

$$\left(\frac{\rho_2}{1-b\rho_2}\right)^{\gamma} = \left(\frac{\rho_N}{1-b\rho_N}\right)^{\gamma}\left[1+\frac{\gamma-1}{2(1-b\rho_N)^2}\right]^{\gamma/(\gamma-1)} \quad (6)$$

During all of the tests, over the measurement range analysed, the velocity remains sonic because the pressure at the nozzle exceeds the critical one. The sonic nozzle calculation method is therefore valid for the duration of the tests. The coefficient C_d is introduced in the sonic nozzle method to fit the mass flow rate to the one computed using the mass balance (see Figure 4). The value of C_d is determined with the method of sum of squared residuals (SSR). The best value of C_d that fit to the flow rate of mass balance is the one with the lowest SSR value. A logarithmic scale is considered in the graph shown in Figure 4 for a better understanding of the impact of C_d and the mass balance is used to calculate the SSR.

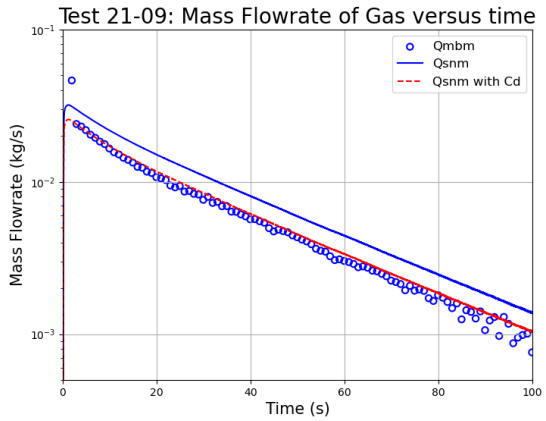

Figure 4. Hydrogen mass flowrate with TPRD of 2mm for the test of 21-09.

The value of C_d obtained from this comparison have been used for other theoretical models (e.g. flame length, radiative heat-fluxes). To summarize all our tank blowdown transient tests of 2021, their Cd values and maximum mass flow rates are given in Table 2. The overestimation of C_d value of 2 mm TPRD during test 21-18 is due to the very short duration of the test.

4.2 Reference jet-fire (200 bar, 2 mm, UP)

The reference test (test 21-09) was performed with a type II cylinder filled with 200 bar of hydrogen. The calibrated orifice used is 2 mm and was oriented vertically upwards. The purpose of this test was to confirm the results obtained in 2020 (test n°20-17) for similar conditions, except for the location in the tunnel.

During test 21-09, an event occured that affected the jet-fire. Despite there being no drop in the mass flow rate, we could not asset an explanation for this phenomenon in the measurements. As shown in Figure 5, the flame clearly widened and decreased in size before 10 seconds, but then returned to a more usual shape.

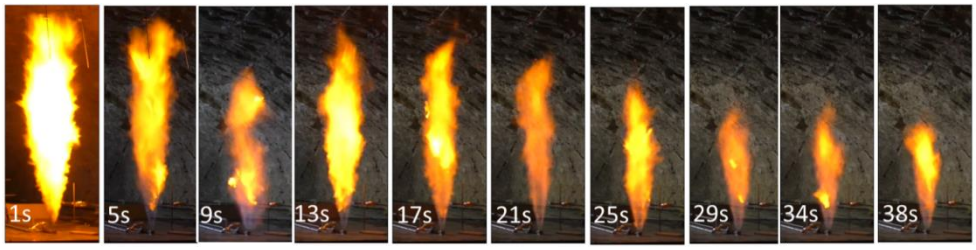

Figure 5. Test 21-09 Morphology of the jet-fire.

The post-processing of the images consequently shows this phenomenon (Figure 6 a) while the theoretical analysis performed using the method described in [1] predicts a monotonic behaviour of the visible flame length. The latter is based on properties derived from the release which does not show any abnormal effect. Due to this unexpected experimental behaviour, it is difficult to conclude on the ability of the theoretical model to predict our results. However, after 20 seconds, the agreement is very good. The results of the same test in 2020 (test 20-17) showed a slower flame length decay. This was due to the use of a commercial TPRD with a smaller discharge coefficient (C_d~0.6).

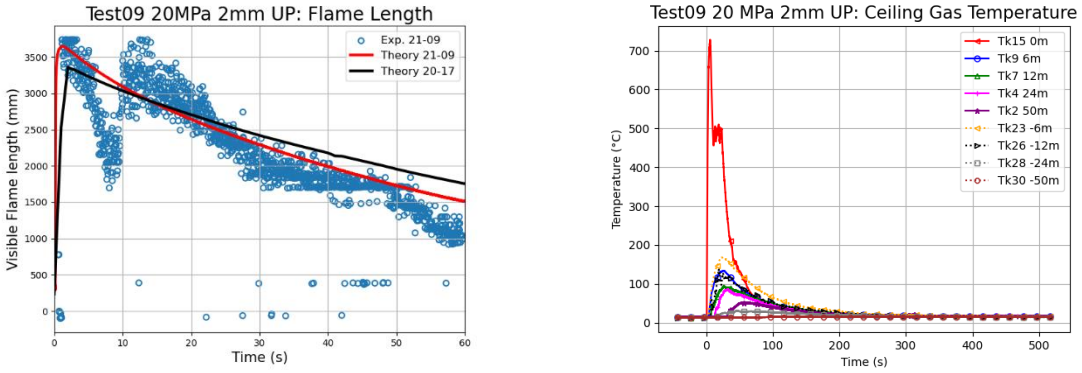

a) b)

Figure 6. Test 21-09 a) Visible flame length with comparison to theory in open environment, b) hot gas temperature close to the ceiling.

As the flame is affected, so are all other quantities (radiated flux and temperatures - Figure 7). The maximum flux was measured by the Fx6 radiometer which was located at a distance of about 2 m from the centre of the flame. For the 2021 test, the measured flux was higher (3.0 kW/m²) whereas in the 2020 test at the same distance a maximum of 2.5 kW/m² was measured (Fx4). Then, the value of 1 kW/m² was reached after about 40 seconds which was comparable in both series of tests. Comparing the fluxes predicted by a point or multi-point radiant source method [10], the predicted values are close to the measurements.

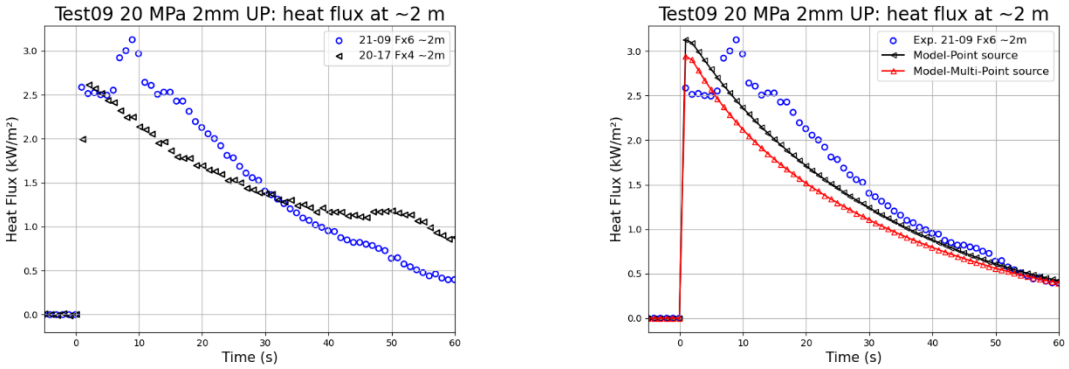

a) b)

Figure 7. Test 21-09: a) Measured Radiated heat flux, b) Radiated heat flux computed by the point and multi-point source theory

For the gas temperature (Figure 6 b), up to 700°C was measured close to the ceiling above the jet-fire, which was comparable to the value measured in 2020. Furthermore, the lateral extension of the hot gas cloud shows a decay below 150°C at 6 m on each side of the tunnel. Due to the irregular rock vault, the decay is less symmetrical than it was under the concrete vault. The back-layering is observed because the natural ventilation of the tunnel during this test was from Autrans (positive Y) to Montaud (negative Y).

4.3 Effect of tank pressure for a 2 mm jet-fire

In test 21-10, the initial driving pressure was around 60 MPa with the same release diameter of 2 mm. The jet-fire shows a monotonic behaviour (Figure 8), which supports the hypothesis of a one-time defect in test 21-09.

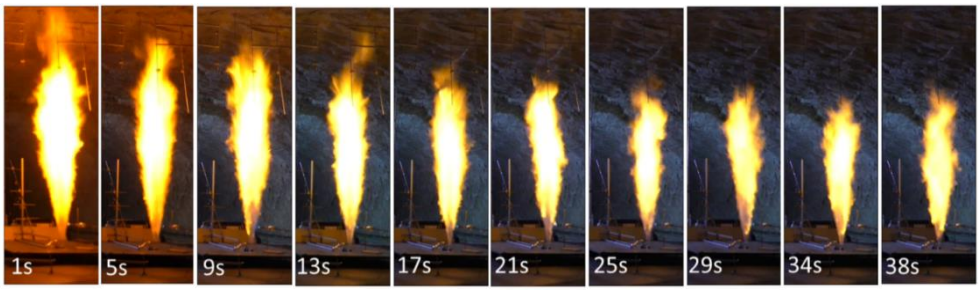

Figure 8. Test 21-10 Morphology of the jet-fire.

The flame had not reach the vault (Figure 8) and this result is confirmed by the theoretical predictions (Figure 9 a). The measurements and the theoretical predictions are in very good agreement with a slight overestimation for the theoretical values which confirms the applicability of theory by Molkov and Saffers [1] to hydrogen safety studies in confined geometries without impingement of the flame.

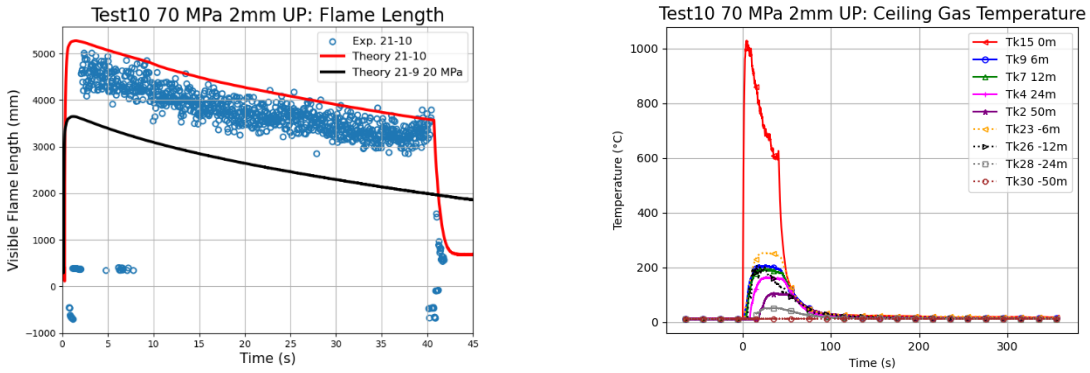

a) b)

Figure 9. Test 21-10 a) Visible flame length with comparison to theory in open environment, b) hot gas temperature close to the ceiling.

During the 2021 tests, the injection solenoid valve was closed when the temperature at the T_1 thermocouple reaches about -50°C, in order to avoid unexpected closure of this solenoid valve. In this test, the initial pressure in the tank, which was about 60 MPa, was close to 18 MPa at the switch-off which occurred about 40 seconds after the opening.

The measured radiated heat fluxes (Figure 10 a) were about 0.5 kW/m² higher than those measured during the 20 MPa jet-fire. The predicted value by the point or multi-point source methods is framed by the measurements at points Fx4 and Fx5 (Figure 10 b). As a reminder, the calculations are made with the half flame length as the reference point for the emission. The difference between these two measurements concerns the elevation of the sensor, which was about 2 m for Fx4 and 0.7 m for Fx5. As a result, at the beginning of the release, the flame is very large and the measurements and calculations are closer for Fx4 and at the end of the release, for a smaller flame, for Fx5.

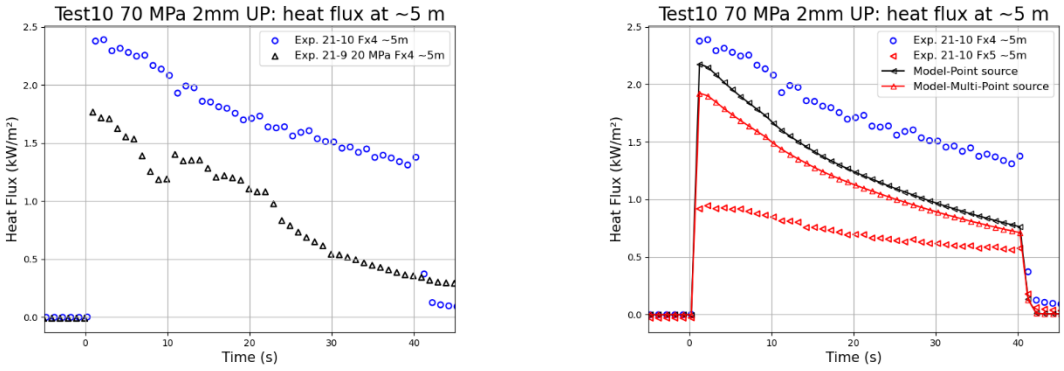

a) b)

Figure 10. Test 21-10: a) Measured Radiated heat flux, b) Radiated heat flux computed by the point- and multi-point source theory

For gas temperatures (Figure 9 b), 1000°C were measured at the tip of the flame. The hot gas temperature was near 300°C at -6 m with the same dissymmetry. If this value is considered as a threshold value for damage to ventilation systems a safe distance of about 6 m is only available. Finally, a temperature close to 200°C was measured at 12 m on each side of the tunnel.

4.4 Effect of release location for a 2 mm jet fire

If at the time of the accident the FCHV do not overturn, the release through the TPRD is oriented downward. In the reference situation, a jet-fire through a 2 mm hole oriented at 45° towards the rear of the vehicle was considered (test 21-12).

The images (Figure 11) show that the lateral extent of the jet flame is about the size of the chassis (about 2 m). Along the rear side of the car (at the opposite of the tank), painted lines on the road allow a rough estimation of the jet flame extension. Each tick is separated by 500 mm and the first one is located 1000 mm far from the release orifice. Consequently, at 1 s, the extent was about 3.5 m and it decreased to about 2.5 m at 29 s.

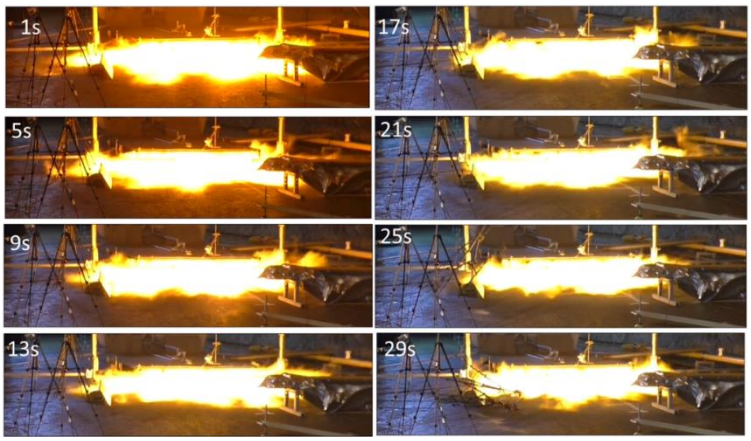

Figure 11. Test 21-12 2 mm DW 45°: Jet-fire morphology viewed from the rear side.

Regarding radiometers measurements (Figure 12 a), the ones located on the chassis were very far from the flame and only provide values around 1 kW/m². Two radiometers installed nearby the flame (Fx5-Fx7) had similar positions and the only difference was their orientation: one was looking horizontally (Fx7) and the second one was looking to the ground where the flame was supposed to be (Fx5). Measurements show that at these distances (5.4 m) and for an impinging flame, the orientation is not a dominant factor but the heat flux reaches the threshold value for first degree burns. However, the shapes of the signals with two peaks is quite unusual. Looking at all the measurements and the video, the

injection flow rate decreases sharply at the start of the injection and then rises again at around 10 seconds. This may explain the behavior of the jet-fire.

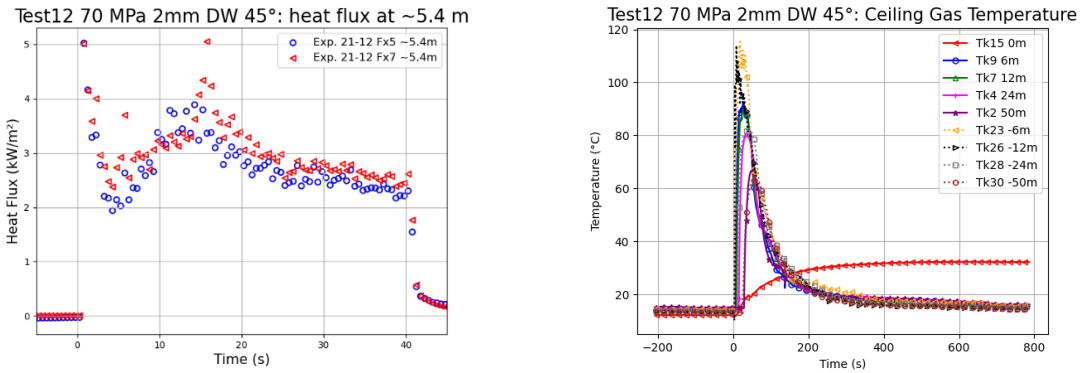

a) b)

Figure 12. Test 21-12: a) Measured Radiated heat flux, b) Gas temperature along the ceiling.

Finally, the hot gas temperatures (Figure 12 b) measured close to the ceiling of the tunnel were below 100°C.

In test 21-18, a downward jet-fire oriented normally to the road (90°) was performed. During this test, a loud sound was heard corresponding to an explosion at the beginning of the ignition. Unfortunately, no pressure sensors were installed to record the overpressures. The pilot flame was installed at the same location from previous tests (Test 21-12 and Test 21-13). The only difference was that the steel plate, which was installed on the road to limit the burning of the asphalted road was highly deformed by the two previous tests. A possible deflection of the jet by the plate toward the front of the car can delay the increase of hydrogen concentration nearby the pilot flame and consequently delay the ignition. However, the video taken during the test shows that 7 images (280 ms) were recorded between the beginning of the release and the fireball. The estimated injection flowrate is around 75 g/s, which leads to 21 g of hydrogen release before the ignition. After the initial explosion, the shape of the flame is very impressive (Figure 13 a) and surrounds the chassis on the four sides with large flames. Despite the thermal protection installed around the high-pressure tank, it was decided to stop the release after 14 seconds.

a) b)

Figure 13. a) Test 21-18 2 mm DW 90°: Jet-fire shape viewed from the rear side, b) Test n°20-22 2 mm DW 90°: Jet-fire morphology viewed from the rear side.

The measured radiative heat fluxes (up to 20 kW/m²) are very high at the beginning due to the fireball especially for the radiometer installed along the chassis on the side of the road (Fx5). At the same time, a peak of temperature of 150°C was measured on the top part of the tunnel at +6 m which corresponds

to the front part of the vehicle (close to the tank in the experimental device) where the huge flames were observed (Figure 13 a).

Finally, the shape of the flame of test 21-18 is compared to the same test performed in 2020 with only 20 MPa in the tank (test n°20-22). With only 20 MPa of driving pressure the extent of the flame was completely modified (Figure 13 b) and the flame mostly stayed under the chassis during the blowdown.

4.5 Effect of release diameter in case of downward 45° jet-fire

To conclude the series of jet-fire tests, the effect of the discharge orifice diameter was studied for a 45° orientation towards the rear of the vehicle. A discharge orifice of 1 mm (test 21-13) leads to a lower extent of the jet-flame (Figure 14). The axial extent is limited to 2.5 m and it seems to stay at this location during the first 30 seconds of the release.

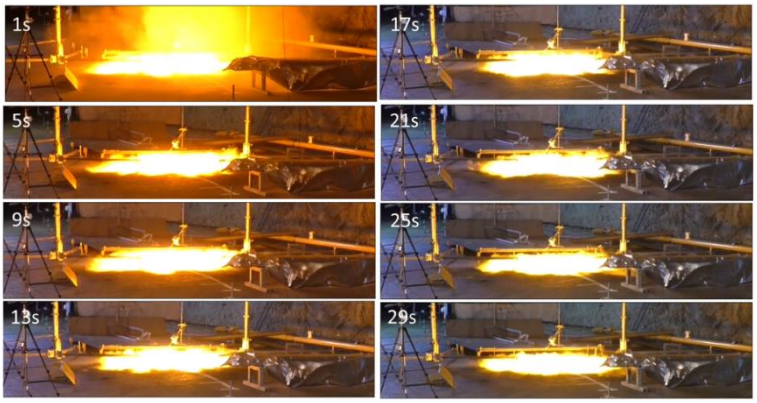

Figure 14. Test 21-13 1 mm DW 45°: Jet-fire morphology viewed from the rear side.

A specific behavior was recorded by the radiometer located close to the jet-fire (Fx5 Figure 15 a). After a first decrease of the radiated heat flux, a sudden increase was recorded from 20 to 50 seconds. Coming back to the video, at this time the jet-flame starts to be thicker. The release parameters were smoothly varying and the pressure was still above 300 bar. A possible explanation is that the asphalted road starts to release burnable products that feed the jet-fire. At the end of the release, the road was on-fire close to the impingement point. The measured gas temperature along the ceiling of the tunnel (Figure 15 b) were below 75°C.

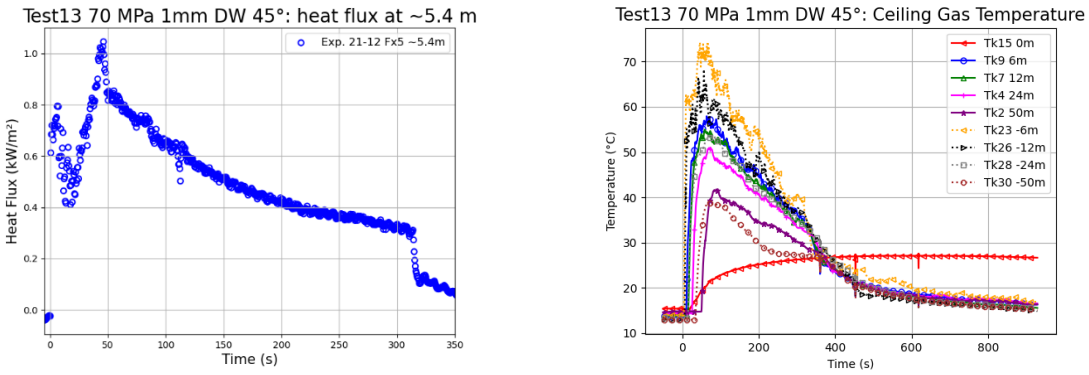

a) b)

Figure 15. Test 21-13: a) Measured Radiated heat flux, b) Gas temperature along the ceiling.

4.6 Coupling Fire/jet-fire for a 2 mm upward jet-fire

Test 21-15 was dedicated to the interaction between the vehicle fire and the jet-fire. An orifice diameter of 2 mm was chosen and the discharge was upwards. Before initiating the release, the propane burner

was ignited (localized and engulfing sections) for approximately seven minutes at the maximum power to stabilize the flow conditions from this fire.

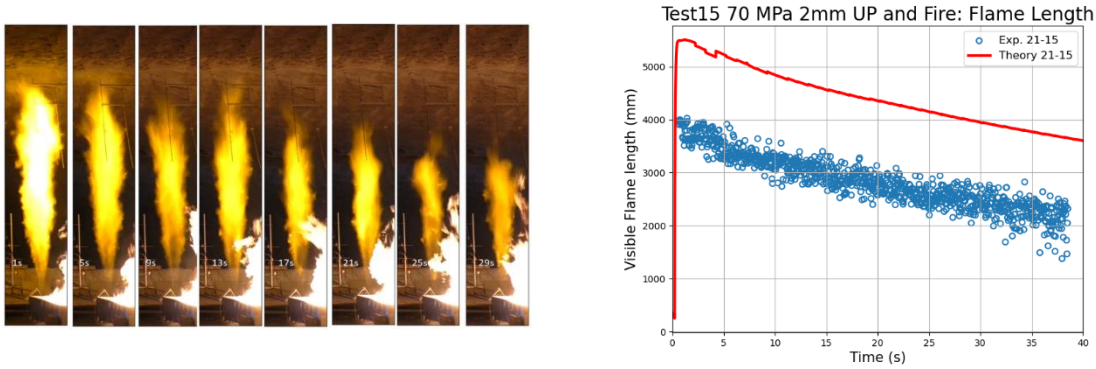

Figure 16. Test 21-15: a) Jet-fire morphology viewed from the rear side, b) Visible flame length with comparison to theory in open environment.

The jet-fire remains well below the tunnel vault and decreases almost continuously (Figure 16 a). Post-processing of the images shows that the flame height is well below the theoretical prediction (Figure 16 b) but also below the values measured in the absence of fire (Test 21-10 Figure 9). Conversely, the videos and measurements do not allow us to conclude on any effect on the fire produced by the burner. Another reason for the jet fire length reduction may be the presence of air cross-flow due to entrainment of air into the burner.

The radiometers (Figure 17 a) show an increase in the radiative flux received when the jet-fire is present. The net radiative effect of adding the jet-fire is not simply a superposition of radiative sources. An amplification of 50% is measured whatever the position of the sensor in relation to the two radiative sources. Steam is probably responsible of such behavior. The temperature of the hot gases (Figure 17 b) at the vault also highlights the effect of the jet-fire. Values close to 250°C were measured in the direction of Autrans up to +24 m. The heat release rate (HRR) of the fire was about 1.5 MW and the jet-fire produced between 9 and 2.5 MW during the blow-down.

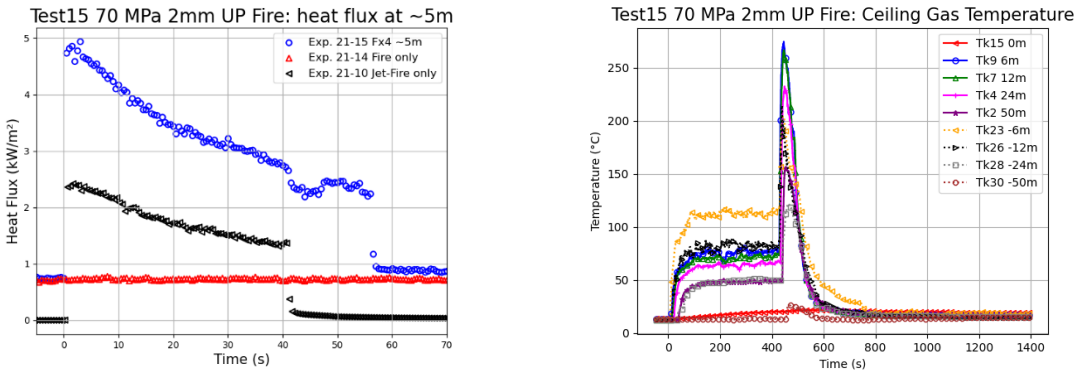

a) b)

Figure 17. Test 21-15: a) Measured Radiated heat flux, b) Gas temperature along the ceiling,

5.0 Conclusions and recommendations

Large scale jet-fire and fire/jet-fire interaction under 70 MPa driving pressure were performed in the Mortier road tunnel. The releases through calibrated orifices occurred downward or upward to simulate the opening of a TPRD with or without the rollover of the damaged car. Experiments show that jet-fires up to 2 mm in release diameter have a small impact on the tunnel (height above 5 m). Lower release

diameters e. g. 1 mm are preferable because they lead to a strong reduction of the jet-fire extend but the jet-fire stays longer, and an asphalted road can be set on fire. Consequently, the nozzle diameter is an important parameter and should be designed for vehicle on-board hydrogen tanks with a diameter as low as reasonably possible. Flame length for vertical jet-fire can be predicted by correlations developed for open environment if the height under the vault is sufficient to develop it. The extent of downward jet-fires oriented 45° towards the rear of the car have been measured up to 3.5 m for the 2 mm diameter. A downward release perpendicular to the road leads to very large flames all around the chassis. Consequently, 45° orientation to the rear showed better performance into the reduction of hazard distances for people and damage to structure. Hot gas cloud (T>300°C) is monitored close to the ceiling of the tunnel in the case of 2 mm release with a car fire (1 MW/m²). This car fire set-up prior the orifice opening lower the extent of the jet-fire and amplify the radiated flux.

6.0 Acknowledgements

HyTunnel-CS project has received funding from the FCH2 JU under grant agreements No.826193. This Joint Undertaking receives support from the European Union's Horizon 2020 research and innovation programme, Hydrogen Europe and Hydrogen Europe Research.

References

[1] V. Molkov and J.-B. Saffers, "Hydrogen jet flames," *Int. J. Hydrog. Energy*, vol. 38, no. 19, pp. 8141–8158, Jun. 2013, doi: 10.1016/j.ijhydene.2012.08.106.
[2] R. W. Schefer, T. C. Houf W. G. and Williams, B. Bourne, and J. Colton, "Characterization of high pressure, underexpanded hydrogen-jet flames," *Int. J. Hydrog. Energy*, vol. 32, no. 12, pp. 2081–2094, 2007.
[3] C. Proust, D. Jamois, and E. Studer, "High pressure hydrogen fires," *Int. J. Hydrog. Energy*, vol. 36, no. 3, pp. 2367–2373, 2010.
[4] E. Studer, D. Jamois, S. Jallais, G. Leroy, J. Hébrad, and V. Blanchetière, "Properties of large-scale hydrogen/methane jet fires," *Int. J. Hydrog. Energy*, vol. 34, no. 23, pp. 9611–9619, 2009.
[5] E. E. Arens, R. C. Youngquist, and S. O. Starr, "Intensity calibrated hydrogen flame spectrum," *Int. J. Hydrog. Energy*, vol. 39, no. 17, pp. 9545–9551, 2014.
[6] J.-L. Consalvi and F. Nmira, "Modeling of large-scale under-expanded hydrogen jet fires," *Proc. Combust. Inst.*, vol. 37, no. 3, pp. 3943–3950, 2019.
[7] B. J. Lowesmith and G. Hankinson, "Large scale high pressure jet fires involving natural gas and natural gas/hydrogen mixtures," *Process Saf. Environ. Prot.*, vol. 90, no. 2, pp. 108–120, Mar. 2012, doi: 10.1016/j.psep.2011.08.009.
[8] H. Mashhadimoslem, A. Ghaemi, A. Palacios, and A. H. Behroozi, "A new method for comparison thermal radiation on large-scale hydrogen and propane jet fires based on experimental and computational studies," *Fuel*, vol. 282, p. 118864, 2020.
[9] A. Molina, R. W. Schefer, and W. G. Houf, "Radiative fraction and optical thickness in large-scale hydrogen-jet fires," *Proc. Combust. Inst.*, vol. 31, no. 2, pp. 2565–2573, 2006.
[10] G. Hankinson and B. J. Lowesmith, "A consideration of methods of determining the radiative characteristics of jet fires," *Combust. Flame*, vol. 159, no. 3, pp. 1165–1177, Mar. 2012, doi: 10.1016/j.combustflame.2011.09.004.
[11] K. Zhou and J. Jiang, "Thermal radiation from vertical turbulent jet flame: line source model," *J. Heat Transf.*, vol. 138, no. 4, 2016.
[12] D. Cirrone, D. Makarov, M. Kuznetsov, A. Friedrich, and V. Molkov, "Effect of heat transfer through the release pipe on simulations of cryogenic hydrogen jet fires and hazard distances," *Int. J. Hydrog. Energy*, vol. 47, no. 50, pp. 21596–21611, 2022.
[13] M. Carboni *et al.*, "Experimental and numerical characterization of hydrogen jet fires," *Int. J. Hydrog. Energy*, vol. 47, no. 51, pp. 21883–21896, 2022.
[14] Y. Xie, N. Lv, X. Wang, D. Wu, and S. Wang, "Thermal and fire characteristics of hydrogen jet flames in the tunnel at longitudinal ventilation strategies," *Fuel*, vol. 306, p. 121659, 2021.
[15] D. Bouix *et al.*, "Full-scale tunnel experiments for fuel cell hydrogen vehicles: jet fire and explosions," presented at the ICHS 2021, Edinburg, Scotland, 2021.